

2017

## Low-Density Self-Driven Electromagnetic Wheel: Comparison of Different Tracks

Nathan GR Gaul

*Northern Virginia Community College*, nrg2990@email.vccs.edu

Walerian Majewski

*Northern Virginia Community College*, wmajewski@nvcc.edu

Follow this and additional works at: <http://commons.vccs.edu/exigence>



Part of the [Engineering Physics Commons](#), and the [Other Physics Commons](#)

---

### Recommended Citation

Gaul, N. G., & Majewski, W. (2017). Low-Density Self-Driven Electromagnetic Wheel: Comparison of Different Tracks. *Exigence*, 1 (1). Retrieved from <http://commons.vccs.edu/exigence/vol1/iss1/9>

This Article is brought to you for free and open access by Digital Commons @ VCCS. It has been accepted for inclusion in Exigence by an authorized editor of Digital Commons @ VCCS. For more information, please contact [tcassidy@vccs.edu](mailto:tcassidy@vccs.edu).

## Low-Density Self-Driven Electromagnetic Wheel: Comparison of Different Tracks

### **Introduction**

The goal of this project is to use a rotating array of powerful magnets to exert levitation and propulsion forces on a conductive metal plate with no direct physical contact between the wheel and the plate. Such a system, usually called an electrodynamic wheel, has a wide variety of practical applications (Bird, Lipo, 2003). The most obvious application is to transportation systems, in which a vehicle could be outfitted with several electrodynamic wheels and then placed over a conductive track or road surface. When those wheels are spun at a sufficient rotational speed, the vehicle would both levitate over the road surface and propel itself forward, all without needing to physically come into contact with the road surface. This lack of direct contact means that there would be no friction and therefore no inefficiency due to friction.

### **Construction of the Wheel**

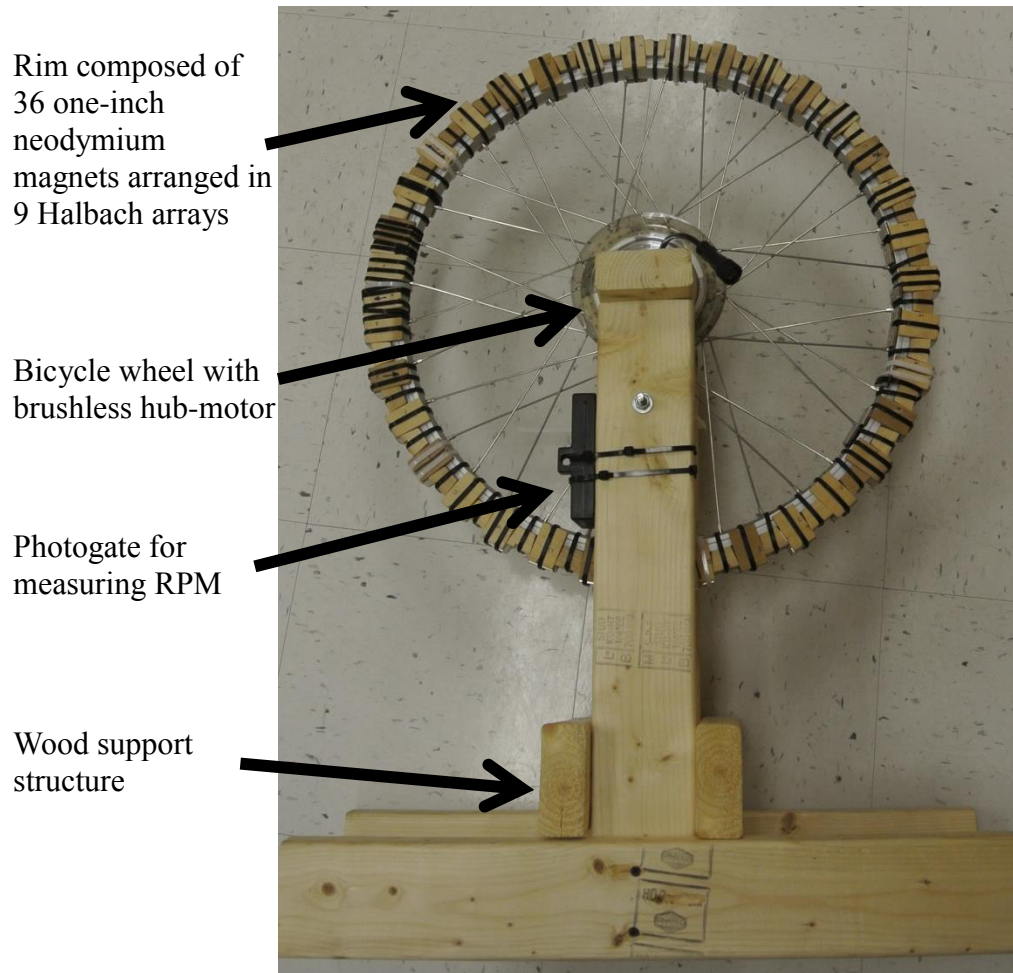
The electrodynamic wheel for this experiment was built around a twenty-inch motorized bicycle wheel. One-inch cube neodymium magnets were spaced around the rim of the wheel approximately one inch apart. A total of 36 magnets were attached to the wheel using small wooden blocks as spacers and plastic ties to secure everything in place. Each magnet had to be oriented so that 9 four-

magnet Halbach arrays were formed around the rim of the wheel with the strong magnetic field being directed outward from the wheel (Halbach, 1985).

The diagram below, using the tip of the arrow to represent the north pole of a magnet, indicates the magnet orientations required to form a Halbach array.

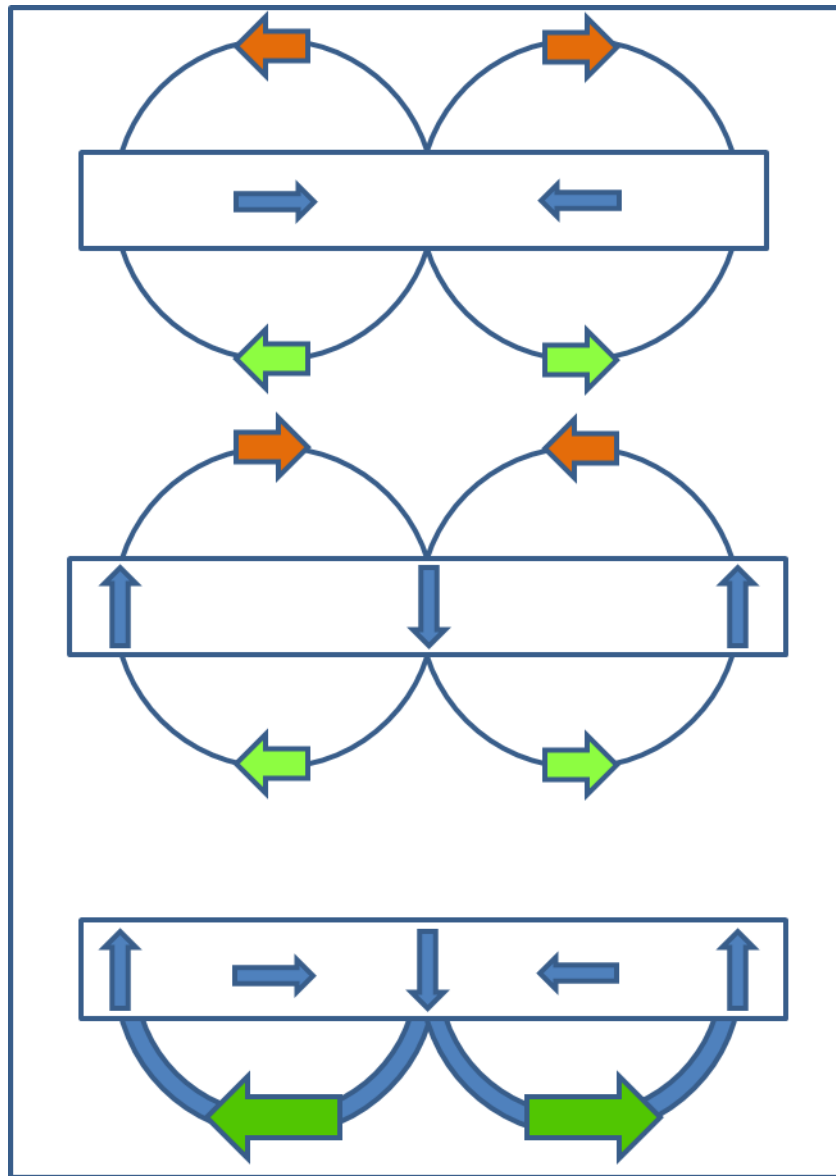


After the magnets were securely mounted to the wheel, a basic wooden support structure was built to hold it upright. A photogate sensor was attached to the frame as well. A small metal plate was taped to two of the spokes and angled so that it would trigger the photogate sensor once per revolution of the wheel. Collecting this data allowed the speed of the wheel to be determined. The completed wheel and support structure is shown below.



### Basic Theory

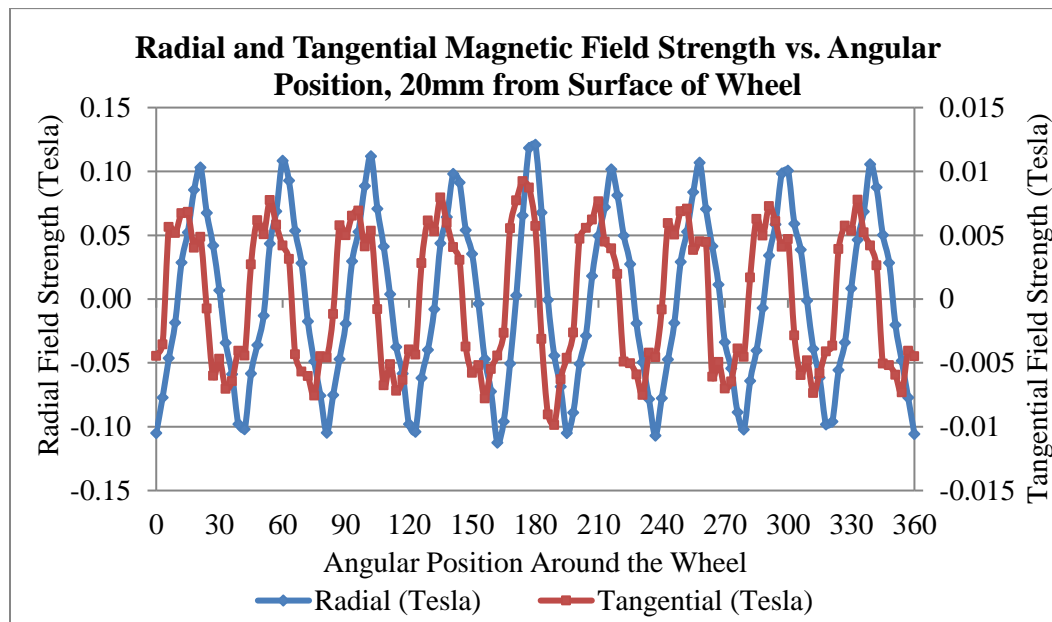
The primary concept involved in the creation of lift and drag forces using this setup is that a changing magnetic field will induce a current in a conductive material (Halbach, 1985). Arranging the magnets into Halbach arrays creates magnetic fields as shown below.



The blue arrows within the rectangle indicate the orientations of the magnets. The tip of the arrow is a north pole and the tail of the arrow is a south pole. When the first two diagrams are superimposed, an amplified magnetic field,

indicated by the large darker green arrows, is created on one side of the array. This field was created by the addition of the fields represented by the small light green arrows. The fields represented by the small red arrows end up canceling each other out when the two diagrams are superimposed to form a Halbach array. This drawing was adapted from the original drawing by J.C. Mallinson (1973).

The graph below shows the radial and tangential components of the magnetic field around the wheel at a distance of 20 mm from the surface. Radial field strength is shown in blue and tangential field strength is shown in red. Some of the abnormalities in the shape of the graph, especially with the tangential component, may be explained by the spaces in between the magnets that make up the Halbach arrays on the wheel.



When a wheel with such a magnetic field is spun, a fixed point near the rim of the wheel will experience rapidly changing magnetic flux. This point would experience increasing magnetic flux in one direction, then decreasing flux in that same direction, then increasing magnetic flux in the opposite direction, and then decreasing magnetic flux in that opposite direction. If a conductive material, such as a copper plate, is put in this area of changing magnetic flux, electrical currents are induced in the plate. These eddy currents create their own magnetic fields that oppose the change in the fields of the permanent magnets on the wheel. The result of these induced currents and their associated magnetic fields is a net lift force and a net drag (or propulsion, depending on the perspective) force.

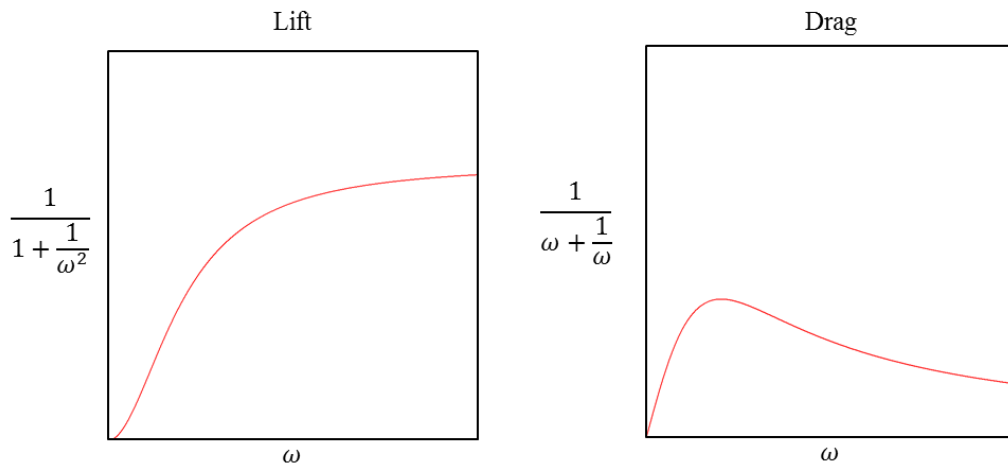
R.F. Post and D.D. Ryutov (2000) developed equations to describe these lift and drag forces. Induced voltage  $V$  and current  $I$  in the plate of effective inductance  $L$  and resistance  $R$  from variable magnetic flux of amplitude  $\Phi_0$  in relative motion with velocity  $v$  (for a linear Halbach array) are related by the circuit equation:

$$V = L \frac{dI}{dt} + RI = \omega \Phi_0 \cos \omega t \quad (1)$$

In our case of rotational motion, the oscillation frequency of the field is  $\omega = n\Omega$ , where “ $n$ ” is the number of Halbach units around the wheel (9 in our wheel) and  $\Omega$  is the angular velocity of the wheel in radians per second.

Complex functions for the lift and drag forces exerted by the wheel on the plate can be developed as functions of several variables. Theoretical prediction for

forces as functions of  $\omega$  for a linear track and Halbach, with rectangular coils as the inductive track, states that at large  $\omega = 9\Omega$  the lift force attains its maximal value, and the drag force drops to zero:



When the ratio of the expression for the lift force and the drag force is taken, the result is a simple linear relationship between the lift to drag ratio and the speed of the wheel:

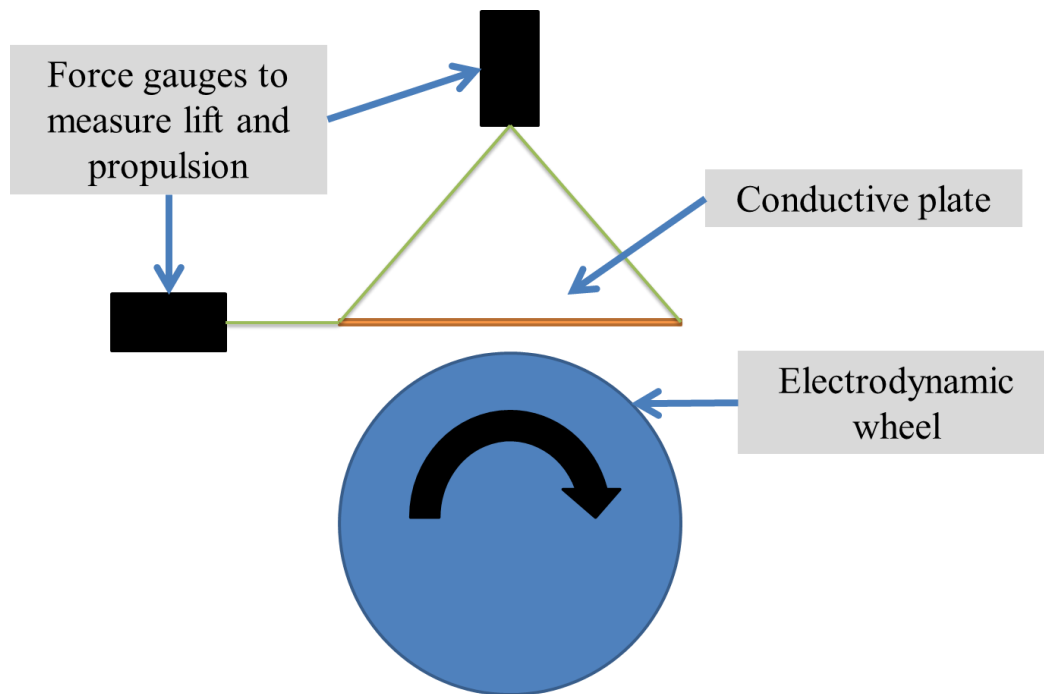
$$\frac{Lift}{Drag} = \frac{\omega L}{R} = \frac{9\Omega L}{R} \quad (2)$$

In the above equation  $\omega$  represents the rate at which the magnetic field oscillates,  $L$  represents the inductance of the plate,  $R$  represents the effective resistance of the circuit the induced current flows through, and  $\Omega$  is the angular velocity of the actual wheel. This is multiplied by the number of north pole to



south pole transitions per revolution of the wheel (9 in this case) to give the rate at which the magnetic field oscillates,  $\omega$ .

### Experimental Setup and Procedure



The experimental setup uses the electromagnetic wheel, conductive plate, and force gauges as shown above. Additional components not shown in the above schematic are the high-current DC power supply and the photogate sensor used to determine the speed of the wheel. The actual wheel in action is shown below. The thin wooden board between the wheel and the conductive plate was used as a

windshield to keep the air turbulence generated by the wheel from interfering with the conductive plate.



Each conductive plate that we experimented on was suspended approximately 18.5 mm from the surface of the magnets. The peak magnetic field strength at this distance averaged to 0.18 Tesla.

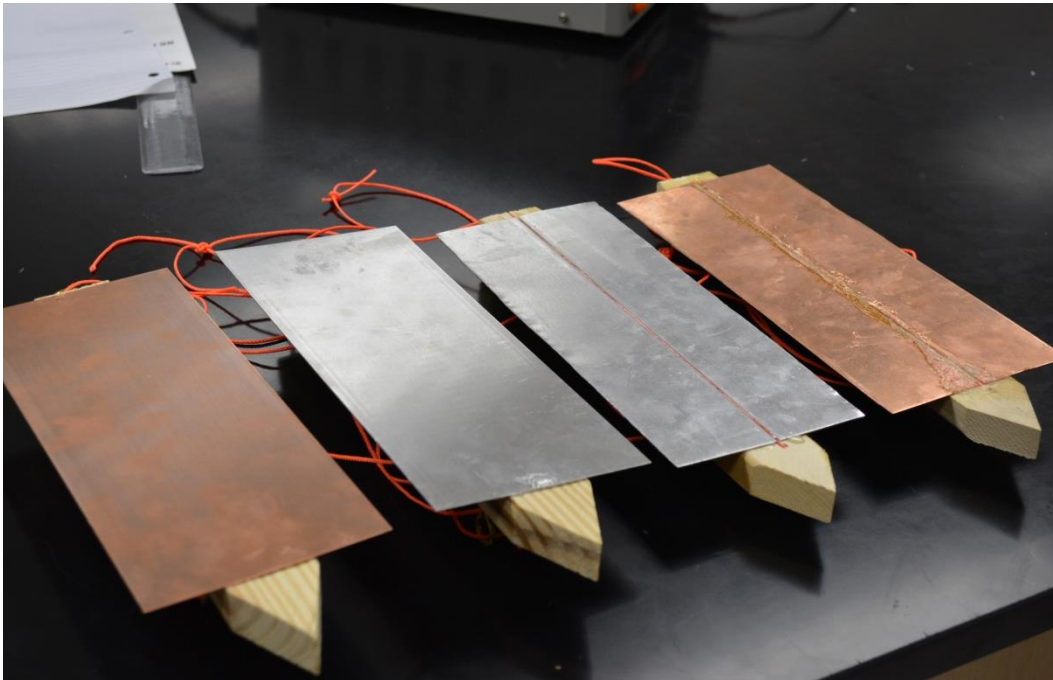
Prior to collecting any data, a significant amount of time was dedicated to ensuring the conductive plate was properly aligned and suspended relative to the wheel. The wheel was then spun up to its maximum speed to verify that the plate was stable and would not wobble excessively or come into contact with anything.

Data was collected using a Vernier LabQuest unit attached to the force gauges and photogate. A polling rate of 250 Hz was used over a two second measurement period. This meant that for each measurement period 500 data points were produced.

Each experimental run started with two baseline measurements during which the wheel was stationary. These measurements provided the starting apparent weight of the plate and the starting amount of force being exerted on the force gauge measuring drag or propulsion. After the completion of the baseline measurements, the external power supply was engaged. Because the motor system in the wheel was originally designed to run off of batteries, it had a low voltage control system installed. This meant that the wheel would only start spinning if more than 21 volts were applied to it. This restriction was meant to prevent over-discharging batteries. To gain finer voltage control, this experiment used an external DC power supply.

The starting voltage was 22 volts, which resulted in a wheel speed of roughly 200 revolutions per minute. After the speed of the wheel had stabilized, the LabQuest unit was used to collect data from the force gauges and photogate over the standard two second period. Once the data for that wheel speed was collected, the speed of the wheel was increased. Voltage was increased by an arbitrary amount of one volt, which meant that each successive run was conducted at a wheel speed that was approximately ten revolutions per minute faster.

After each increase in voltage, the wheel speed was allowed to stabilize, and then data was collected over another two second period. This process was repeated until the input voltage reached 40 volts. The wheel typically spun at approximately 370 revolutions per minute at this voltage. Higher speeds were not tested due to concerns regarding overloading the motor.



Experiments were performed with a total of five different conductive plates or “tracks”. The aluminum and copper rectangular plates were both 25.3 cm x 10 cm x 0.6 mm and had masses of 206 g and 283 g respectively. The circular aluminum plate had a diameter of 19 cm, a mass of 200 g, and a thickness of

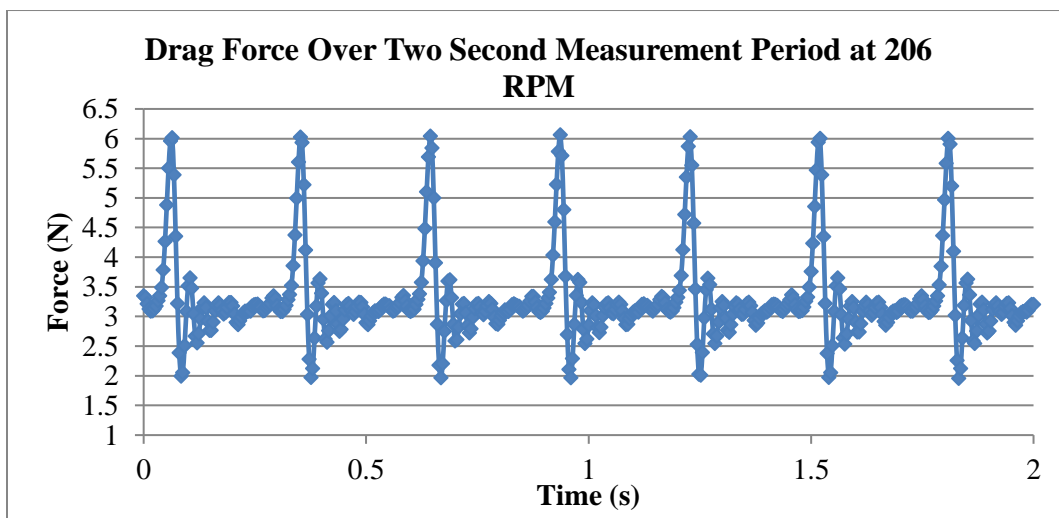
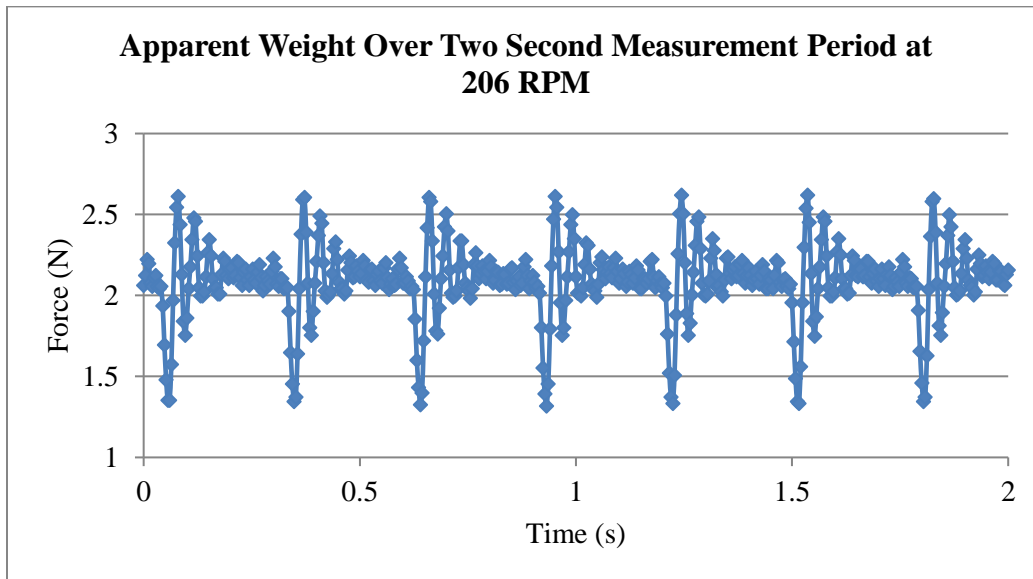
1 mm. Copper and aluminum were chosen as materials so that the effect of different conductivities could be observed. The aluminum disk (which was larger than the aluminum plate) allowed for comparison of the effect of the sizes of the plates on the results. Split tracks were used to investigate the self-stabilizing properties of such a design after lift-off was achieved, as suggested by J. Bird and T. A. Lipo. All the experimental factors except the type of track were kept constant in between runs.

### **Experimental Results**

The rotating magnetic field induces eddy currents in our conducting non-magnetic plates, which are alternately attracted or repelled from the magnets in both normal and tangential directions. The normal force is the lift force that reduces the apparent weight of the plate, while the tangential force is a drag force. While being a hindrance in the linear motion of magnets above a straight track, in our case, this force plays the useful role of the propulsion force. Lift and drag are shifted in phase. Sample graphs of the lift and drag forces at a given wheel speed over time are shown below.

The small oscillations shown in the graph were expected due to the alternate attraction and repulsion of the plate from the wheel. The occurrences of the large spikes in value were caused by a cluster of magnets that were closer together than the others. Rather than being spaced roughly an inch apart, these four magnets

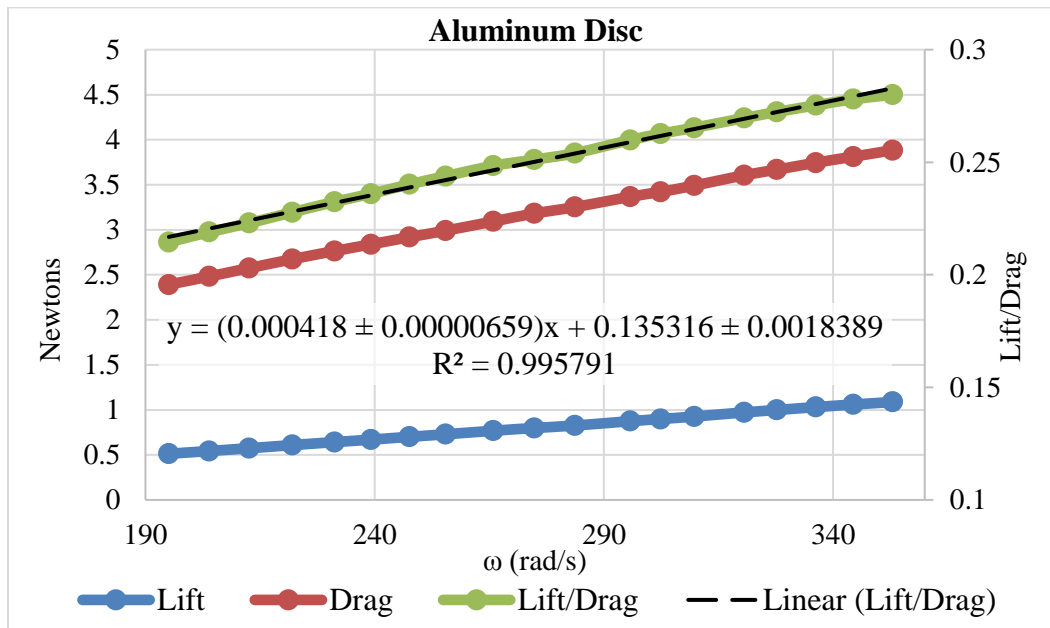
were practically side by side. This increase in density meant a more rapidly changing magnetic field over that distance and therefore more force. The inconsistent spacing of the magnets was a result of a problem with the assembly of the wheel.

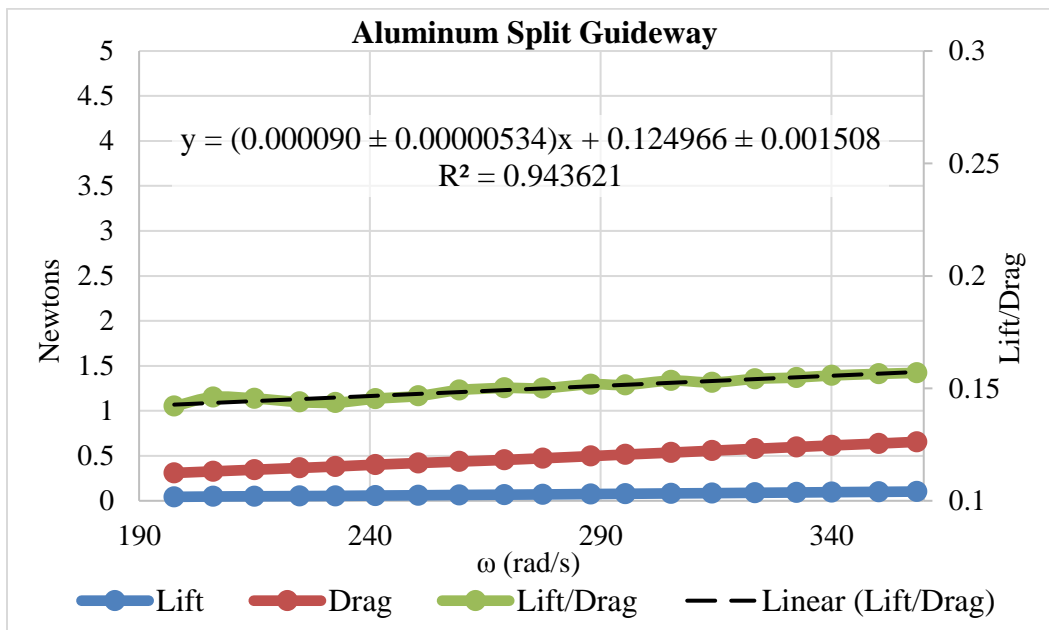
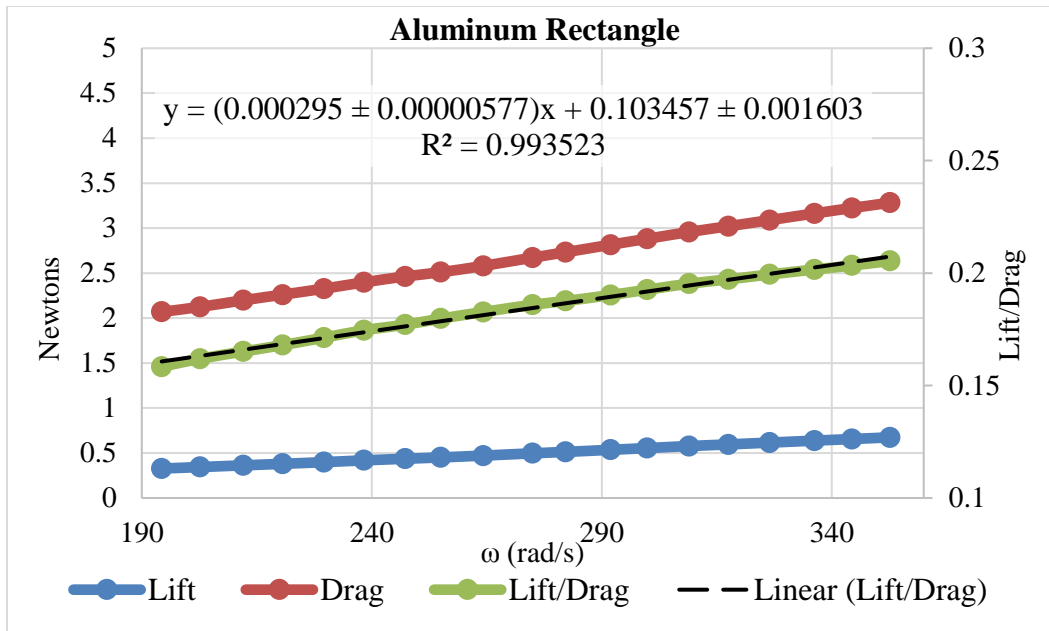


Using a program developed by another researcher in our group, the thousands of data points collected over the course of each experimental run were instantly converted into a collection of average force readings for each wheel speed.

The following graphs present the average lift and drag forces versus the rate at which the magnetic field was oscillating,  $\omega$ . The field oscillated 9 times for every rotation of the wheel. The x-axis represents this field oscillation rate variable,  $\omega$ . The lift to drag ratio was also plotted.

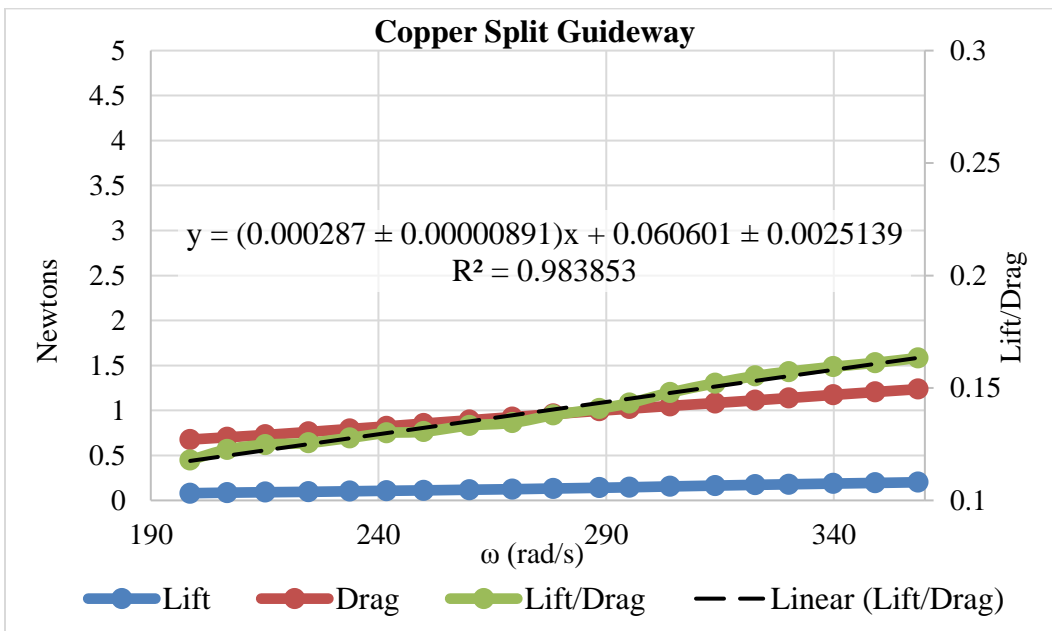
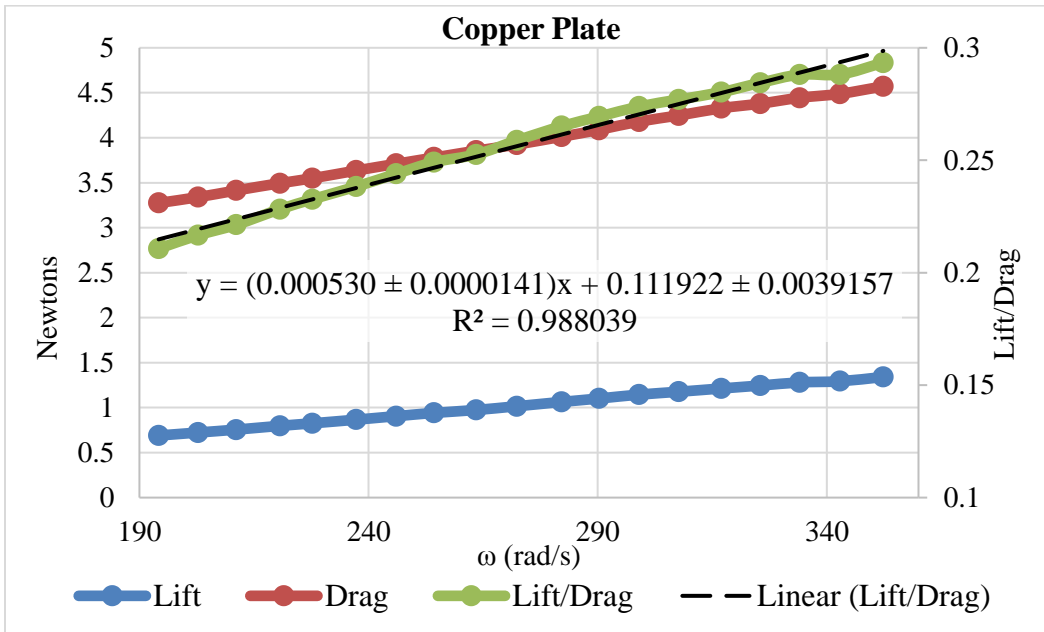
### Lift, Drag, and Lift-to-Drag Ratio for Aluminum Tracks







### Lift, Drag, and Lift-to-Drag Ratio for Copper Tracks



## Discussion

All of the tracks demonstrated a linear relationship between the lift-to-drag ratio and the rate at which the magnetic field oscillated. This linear relationship matched extremely well with the theory. As expected, the copper plate produced more lift and had a higher lift to drag ratio than the aluminum plate because of copper's larger conductivity.

Full lift-off, meaning a lift force greater than the weight of the plate, was not achieved. The most lift was obtained from the copper track, with over 1.3 Newtons of lifting force generated. This was equivalent to approximately 48% of the full weight of the track, or just under one-third of a pound of lift.

As indicated by the graphs, the split tracks, meant to be more stable after lift-off, were extremely inefficient in terms of producing lift. The linear lift-to-drag versus wheel speed relationship remained, but the values of this ratio were extremely small. This inefficiency may be explained by the gap between the two halves of the track, which interrupts the flow of induced currents through the middle of the plate.

Both the copper rectangle and the aluminum rectangle had the same calculated inductance of 111.5 nano-Henries. Cancelling this common value in the ratio of the lift-to-drag ratios for the copper and aluminum tracks at the same  $\omega$ , this ratio must be equal to the ratio of the resistivities  $\rho$  of the two rectangular metal tracks:

$$\frac{(Lift/Drag)_{copper}}{(Lift/Drag)_{aluminum}} = \frac{L/R_{copper}}{L/R_{aluminum}} = \frac{\rho_{aluminum}}{\rho_{copper}} \quad (3)$$

From our data, this calculated ratio turned out to be  $1.80 \pm 0.0355$ . The ratio of these resistivities using the accepted values of the resistivities of copper and aluminum is  $\frac{2.82}{1.68} = 1.68$ . The calculated experimental value compared reasonably well with this accepted value, with the percent difference between the two being less than 10%.

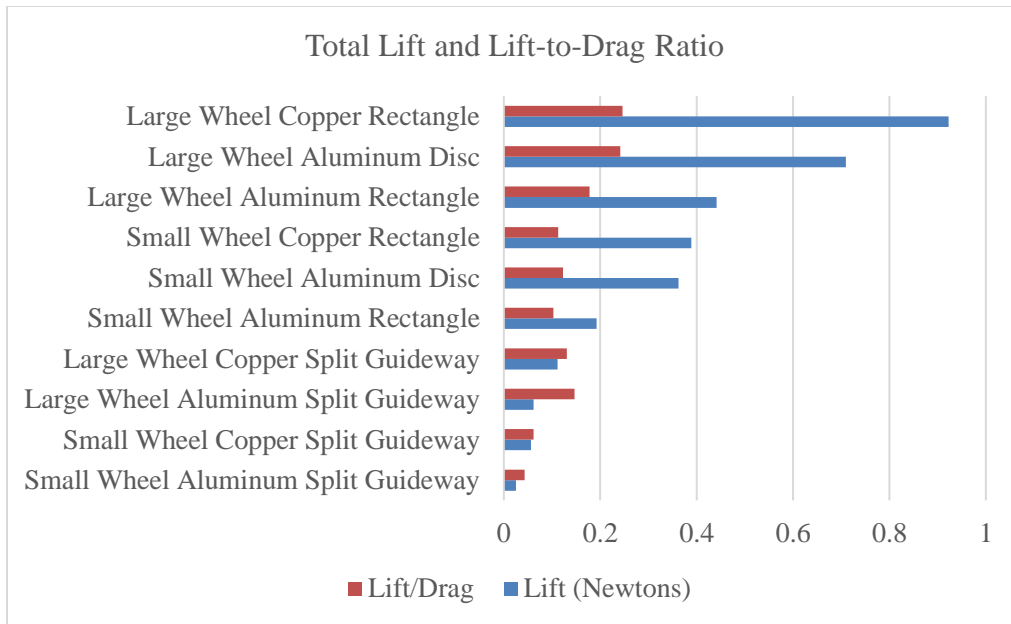
Similarly, the effective resistance experienced by the induced currents in the plates can be calculated using the estimated inductance of 111.5 nano-Henries and the measured lift-to-drag ratios at some  $\omega$ . For the copper plate, the effective resistance  $R$  the induced currents experienced was calculated to be  $0.210 \pm 0.00560$  milli-Ohms. For the aluminum rectangle, the effective resistance the induced currents experienced was calculated to be  $0.378 \pm 0.00739$  milli-Ohms.

### **Comparison of Two Electrodynamic Wheels**

Below, a comparison was made with another experiment in our group.

This experiment used a small electrodynamic wheel, with 12 Nd magnets tightly spaced around the rim in a series of 3 Halbach arrays. As on the large wheel, the arrays were oriented so that the field was amplified on the outside rim.

For comparison, the large wheel has a radius of 28.8 cm and the small EDW has a 5.1 cm radius. The same conductive tracks were used and were placed in an area of 0.18 Tesla maximum field strength of the small wheel, to make the results comparable to that of the large wheel. For the comparison below, the lift and lift-to-drag ratios for all of the plates were compared between the two different wheels at an  $\omega$  value of 250 radians per second, meaning the magnetic field on the outside of the wheels was reversing itself at that rate. Because of the differences in radius and number of magnets, the physical rotational speeds of the wheels were not equal.



### Details of Comparison of Two EDWs

On both wheels the thickness of the magnets in the radial direction was the same, 1 inch or 2.54 centimeters. The total volume of magnets on the large wheel was 36 cubic inches, or 590 cubic centimeters, weighing a total of 9.765 pounds. The total volume of the magnets in the small wheel was 9.42 cubic inches, or 154 cubic centimeters, weighing a total of 2.58 pounds.

The thirty-six magnets on the large wheel were distributed roughly 1 inch apart around the rim, each separated by an angle of approximately ten degrees. The twelve magnets on the small wheel were supported each by an angle of thirty degrees with no spacing between the magnets.

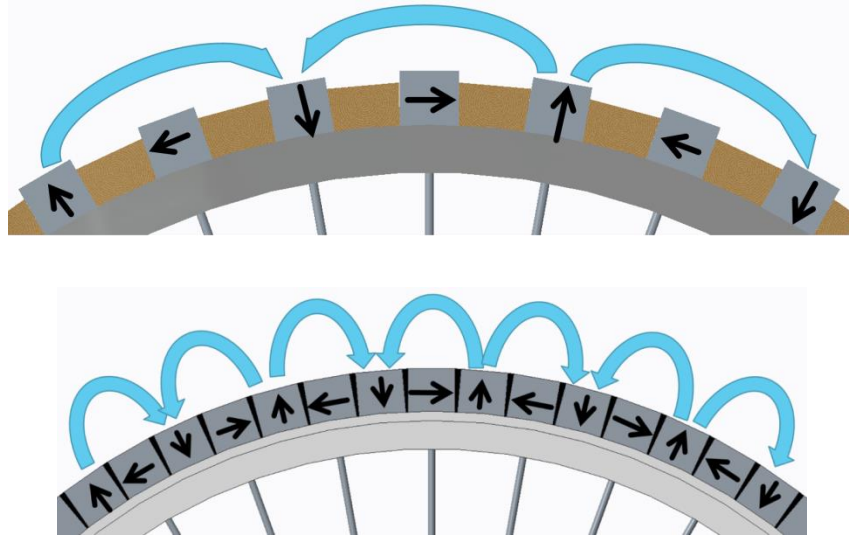
The gap between the plate and the wheel was not the same for the large and small wheels. However, in both cases the plates were suspended at a distance

from the wheel at which the peak magnetic field strength was 0.18 Tesla. This was done to make the data more comparable.

The lift force per unit of magnet volume for the copper plate over the large wheel was 0.00156 Newtons per cubic centimeter at a  $\omega$  value of 250 radians per second. The lift force per unit of magnet volume for the copper plate over the small wheel was 0.00252 Newtons per cubic centimeter, meaning that magnet for magnet, the small wheel produced more lift at a given magnetic field oscillation rate.

### **Proposed Wheel Upgrade**

To improve upon the original project and reach full levitation, a slightly larger wheel will be used and 76 magnets will be placed around the rim, instead of the current 36. The increased number of magnets will increase the number of north to south reversals of the magnetic field per revolution. This will increase the value of  $n$ , equal to the number of Halbach arrays around the wheel, from 9 to 19. Effectively, the wheel will still spin in the same speed range of 200 to 380 revolutions per minute, however, the magnetic field at the point of the suspended plate will oscillate over twice as fast. In addition to the extra magnets, other improvements will be made to the wheel, such as a more secure magnet mounting system. Below is a CAD render showing the current wheel (top) and the design of the proposed upgrade (bottom), with magnetization directions indicated by arrows and the field lines indicated by the blue arcs.



### Applications

The technology demonstrated by this project has potential applications in a variety of areas. Vehicles using electrodynamic wheels would be able to levitate above and propel themselves along a conductive road surface.

Multiple electrodynamic wheels could be placed so that their magnetic fields interact and create non-contact gear coupling systems. Similarly, the electrodynamic wheel can be used to push liquid metal along a pipe or channel, move objects along non-contact conveyor belts, or even launch conductive projectiles.

## References

- Bird, J., T.A. Lipo, (2003). An Electrodynamic Wheel: An Integrated Propulsion and Levitation Machine, University of Wisconsin, Madison, WI, Electric Machines and Drives Conference. IEMDC'03. IEEE International (Volume:3).
- Bird, J., T.A. Lipo, (2005). An Electrodynamic Wheel with a Split-Guideway Capable of Simultaneously Creating Suspension, Thrust and Guidance Forces, University of Wisconsin-Madison, College of Engineering, Wisconsin Power Electronics Research Center, research report 2005-39.
- Halbach, K., (1985). Applications of Permanent Magnets in Accelerators and Electron Storage Rings, *Journal of Applied Physics*, Vol. 67, 109.
- Mallinson, J.C., (December 1973). One-sided Fluxes - A Magnetic Curiosity?, *IEEE Transactions on Magnetics*, Vol. Mag-9 No. 4, p. 1-6.
- Post, R.F., D.D. Ryutov, (2000). The Inductrack Approach to Magnetic Levitation, UCRL-JC-138593 preprint.